PAIN® 155 (2014) 1481–1491

PAIN®

www.elsevier.com/locate/pain

Tear fluid hyperosmolality increases nerve impulse activity of cold thermoreceptor endings of the cornea

Andres Parra [a,1], Omar Gonzalez-Gonzalez [b,1], Juana Gallar [a], Carlos Belmonte [a,b,*]

[a] Instituto de Neurociencias, Universidad Miguel Hernandez-CSIC, San Juan de Alicante, Spain
[b] Fundacion de Investigación Oftalmológica, Instituto de Oftalmología Fernández-Vega, Oviedo, Spain

Sponsorships or competing interests that may be relevant to content are disclosed at the end of this article.

ARTICLE INFO

Article history:
Received 3 October 2013
Received in revised form 14 April 2014
Accepted 22 April 2014

Keywords:
Dry eye
Cornea
Cold thermoreceptors
Polymodal nociceptors
Hyperosmotic stress
Tear osmolality

ABSTRACT

Dry eye disease (DED) is a multifactorial disorder affecting the composition and volume of tears. DED causes ocular surface dryness, cooling, and hyperosmolality, leading ultimately to corneal epithelium damage and reduced visual performance. Ocular discomfort is the main clinical symptom in DED. However, the peripheral neural source of such unpleasant sensations is still unclear. We analyzed in excised, superfused mouse eyes, the effect of NaCl-induced hyperosmolality (325–1005 mOsm·kg^{-1}) on corneal cold thermoreceptor and polymodal nociceptor nerve terminal impulse (NTI) activity. Osmolality elevations at basal corneal temperature (33.6°C) linearly increased the ongoing NTI frequency of cold thermoreceptors, at a mean rate of 0.34 imp·s^{-1}/10 mOsm. This frequency increase became significant with osmolality values greater than 340 mOsm. Comparison of cold thermoreceptor activity increase induced by a dynamic temperature reduction of 1.8°C under iso- and hyperosmolal (360-mOsm) conditions provided evidence that more than 50% of the increased firing response was attributable to hyperosmolality. Comparatively, activation of corneal polymodal nociceptor endings by hyperosmolal solutions started with values of 600 mOsm and greater. Sensitization of polymodal nociceptors by continuous perfusion with an "inflammatory soup" (bradykinin, histamine, prostaglandin E_2 [PGE_2], serotonin, and adenosine triphosphate [ATP]) did not enhance their activation by hyperosmolal solutions. High osmolality also altered the firing pattern and shape of cold and polymodal NTIs, possibly reflecting disturbances in local membrane currents. Results strongly suggest that tear osmolality elevations in the range observed in DED predominantly excite cold thermoreceptors, supporting the hypothesis that dryness sensations experienced by these patients are due, at least in part, to an augmented activity of corneal cold thermoreceptors.

1. Introduction

The ocular surface is covered by the precorneal tear film, a complex gel that maintains moistness of the nonkeratinized epithelium of the corneal surface and conjunctiva [19,24]. In healthy eyes, the aqueous fraction of the tear film evaporates continuously at a rate determined by environmental temperature, relative humidity, and air flow, and is replenished regularly with tears secreted by main and accessory lacrimal glands, thereby maintaining a stable volume and chemical composition of the tear film aqueous layer [15,18,19,39,49,52].

Dry eye disease (DED) has been defined as a multifactorial disease of the tears and ocular surface that is due, in most cases, to tear deficiency or excessive evaporation, which results in symptoms of discomfort and tear instability, with potential damage to the ocular surface [54]. Ocular discomfort is the main clinical symptom in mild and moderate DED [42] and is the result of the excitation of sensory nerve fibers innervating the ocular surface [1,5]. These include mechano-nociceptors that are preferentially activated by mechanical forces; polymodal nociceptors that additionally respond to heat, exogenous irritant chemicals, and endogenous inflammatory mediators; and cold thermoreceptors primarily activated by small reductions of the ocular surface temperature. All functional types of fibers are comparatively more

* Corresponding author at: Instituto de Neurociencias, Universidad Miguel Hernandez-CSIC, Avda Santiago Ramon y Cajal 2, 03550 San Juan de Alicante, Spain. Tel.: +34 96591 9532; fax: +34 96591 9549.
E-mail address: carlos.belmonte@umh.es (C. Belmonte).
[1] A.P. and O.G.-G. contributed equally to this work.

http://dx.doi.org/10.1016/j.pain.2014.04.025

abundant in the center than in the periphery of the cornea, decreasing in density in the bulbar conjunctiva [7,9,14,26].

During DED, disturbances derived from augmented evaporation may act as stimuli for the different functional types of corneal and conjunctival sensory nerve terminals, thereby becoming a potential cause of ocular discomfort [18,48,49]. High tear evaporation rate decreases markedly the ocular surface temperature during interblink periods and accelerates breakup of the precorneal tear film, contributing to mechanical stress, injury of the corneal and conjunctival epithelium, and local inflammation [11,22,28,43,50,58,59]. Each of these disturbances represents a possible stimulus for thermoreceptor, mechano-nociceptor, or polymodal nociceptor corneal nerve terminals [5].

Augmented evaporation also increases electrolyte concentration, raising the osmolality of the tear film [10,48]. Osmolality increases stimulate corneal sensory receptors [7,26,37,38,47,59]. However, the influence of osmolal changes on the impulse activity of the ocular surface sensory afferents has not been analyzed in detail. Osmolality of human healthy tears (300–315 $mOsm \cdot kg^{-1}$) [10,60] is mainly determined by the electrolyte content of the tear film aqueous phase, principally sodium, potassium, chloride, and bicarbonate with a minor contribution of proteins and sugars. Osmolality becomes higher in DED [23,56], rising to mean osmolality values up to 365 mOsm and possibly reaching higher levels in areas of break-up of the precorneal tear layer [16,29,56]. In the present work, we studied whether controlled ocular surface osmolality increases, caused by augmented NaCl concentration as would occur during enhanced evaporation of tears, modify the spontaneous and stimulus-evoked nerve impulse activity of corneal sensory receptor fibers.

2. Methods

2.1. Animals

Male (2–6 months of age) C57BL/6 (n = 44) and ICR (n = 4) mice were used. No statistical differences in the impulse firing characteristics under different experimental conditions were observed between mouse strains, and therefore the data of both strains were pooled.

All experiments were conducted according to the Animal Use Guidelines of the European Community (2007/526/EC) and the Spanish Council for Scientific Research (CSIC); the experiments were approved by the University Miguel Hernandez Animal Care and Ethics Committees and adhered to the guidelines of the Committee for Research and Ethical Issues of IASP.

2.2. Electrophysiological recordings

The procedure for the recording of single corneal nerve terminals in vitro described in previous studies [13,53] was used. In brief, mice were killed by exposure to CO_2. Eyes were removed and maintained for 30 minutes in saline solution of the following composition (in mmol/L): NaCl (128), KCl (5), NaH_2PO_4 (1), $NaHCO_3$ (26), $CaCl_2$ (2.4), $MgCl_2$ (1.3), and glucose (10) at room temperature, bubbled with carbogen (5% CO_2 and 95% O_2). They were subsequently placed in a recording chamber and superfused with saline solution at temperatures adjusted with a servo-controlled Peltier. An Ag/AgCl borosilicate recording pipette (tip diameter, ≈50 μm) filled with the same solution was placed onto the corneal epithelium surface with a micromanipulator. A gentle suction was applied to seal the electrode tip to the epithelium. Nerve terminal impulses (NTI) were recorded and amplified with an AC amplifier (Neurolog NL104, Digitimer, Welwyn, UK), and stored at 10 kHz in a computer using a CED micro1401 interface and Spike 2 software (both from Cambridge Electronic Design, Cambridge, UK). Only recordings containing a single unit, clearly distinguished from noise (≈10 V peak-to-peak) and identifiable by its waveform and firing pattern, were used for further analysis. To avoid deterioration of the preparation with time, duration of the recording periods was restricted to a maximum of 4 hours. We have repeatedly confirmed that 6 to 8 hours after enucleation, the firing characteristics of nerve terminals remain unaltered (unpublished data).

2.3. Experimental protocol

The appearance of spontaneous or stimulus-evoked activity after application of the pipette onto the cornea was used to ascertain the successful location of an active sensory nerve terminal. Responsiveness to mechanical stimulation was assessed with a gentle forward displacement of the micromanipulator holding the recording electrode.

Cold thermoreceptor terminals were easily recognized by the presence of ongoing NTI activity immediately after placing the pipette on the receptive field. Polymodal nociceptors were identified by the occasional occurrence of 1 spontaneous NTI in the 1- to 2-minute period after application of the pipette, absence of response to cooling but clear activation by heating pulses, and firing of 1 or a few NTIs in response to a gentle push with the micromanipulator. Characterization of polymodal nociceptors was confirmed by the positive response to capsaicin (1 μmol/L; see below).

Cold stimulation was performed by decreasing the background temperature of the perfusion solution from 33.6°C ± 0.1°C to 16.9°C ± 0.3°C during a 26-second period. This produced a cooling ramp, dropping at a rate of 0.7°C ± 0.1°C s^{-1}, then returning to basal temperature (Fig. 1A). In a set of experiments involving the recording of cold thermoreceptor terminals, −3°C cooling steps lasting 2.5 minutes from 33.6°C down to 21.6°C were also applied. A minimum period of 5 minutes was allowed between thermal stimuli. For heat stimulation of polymodal nociceptors, warming ramps up to 50.3°C ± 0.2°C at a rate of 0.6°C·s^{-1} were performed.

Chemical stimulation of polymodal nociceptor endings with 1 μmol/L capsaicin was carried out by shifting the perfusion from control saline solution to saline solution containing the drug, which was perfused for 30 seconds at 33.6°C. Application of the drug was followed by a washing period of at least 5 minutes.

After positive identification, cold thermoreceptor and polymodal nociceptor terminals were exposed to solutions of increasing osmolality. In the present study, nerve terminals responding exclusively to mechanical stimulation were not found. Perfusion with control saline solution (mean osmolality measured with a freezing point osmometer = 309.5 ± 0.6 mOsm) was followed by perfusion with different hyperosmolal solutions (ranging from 325 to 1005 mOsm; see below). The mean time of exposure to each hyperosmolal solution at basal temperature was 348 ± 13 seconds. In experiments in which stepwise cooling was applied to cold thermoreceptor terminals, perfusion with high-osmolality solutions was initiated 6 minutes before the onset of the stepwise cooling cycle and was maintained until the temperature returned to basal levels after the last cooling step. A separate group of polymodal units were initially exposed to an "inflammatory soup" (see specifications below) [64] added to the perfusion solution for 5 minutes to mimic sensitization of polymodal nociceptors caused by inflammatory conditions in vivo. Perfusion was continued thereafter with hyperosmolal solutions (370 and 490 mOsm) containing the inflammatory soup.

2.4. Analysis of NTI activity

The following parameters were analyzed in the different classes of sensory terminals.

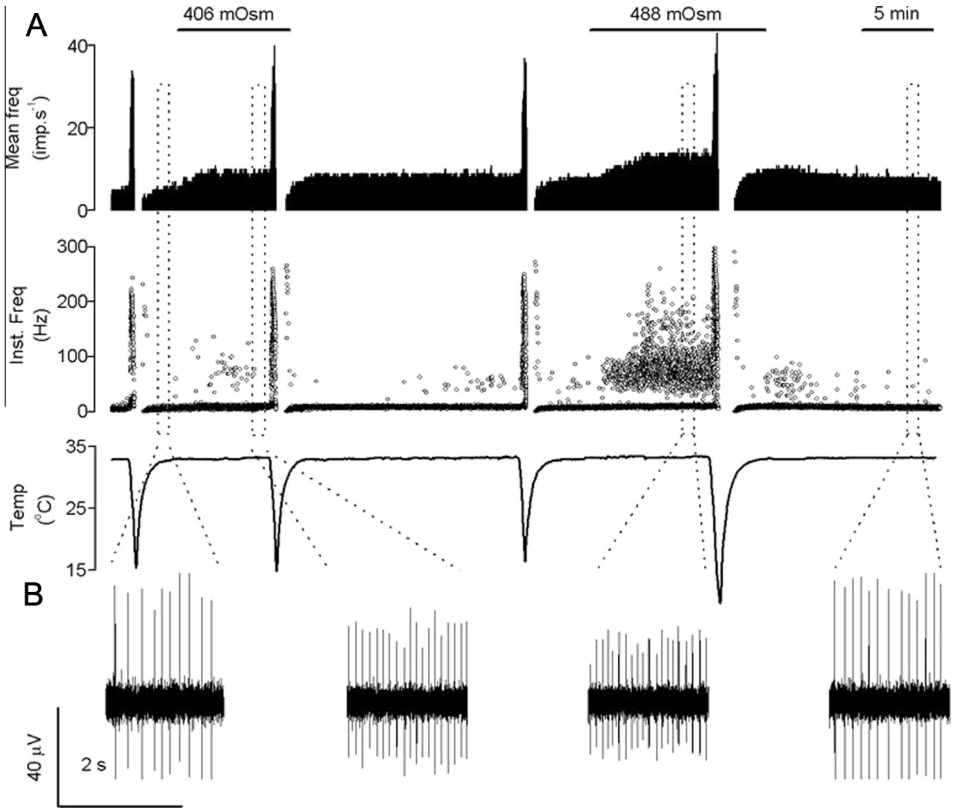

Fig. 1. Relationship between osmolality and cold thermoreceptor activity. (A) Effect of hyperosmolal solutions on the ongoing nerve terminal impulse (NTI) activity at 33.6°C and response to cooling ramps to 15°C of a cold thermoreceptor ending. Upper trace, mean firing rate (imp·s^{-1}); middle trace, instantaneous frequency in Hz; lower trace, bath temperature (°C). (B) Sample recordings are expanded views of the NTIs fired by the ending during the periods marked in A between dashed lines, during the recording in iso-osmolal conditions, during perfusion with 406 mOsm and 488 mOsm solutions, and during the washing period.

2.4.1. Cold thermoreceptors

Spontaneous activity: Mean basal ongoing activity in impulses per second (imp·s^{-1}) at 33.6°C, measured during the minute that preceded the onset of a cooling ramp. *Cooling threshold*: Temperature decrease (°C) at which NTI frequency increased to a value that was the mean NTI frequency measured during the 10-second period preceding the onset of a cooling ramp, plus 3 times its standard deviation. *Mean NTI frequency:* Average number of NTIs recorded per second (imp·s^{-1}). *Peak frequency* (PF): Maximum NTI frequency (in imp·s^{-1}) attained during a cooling ramp. *Mean slope of the response to a cooling ramp* (imp·s^{-1}°C^{-1}): Slope of the line between the value of mean activity at the cooling threshold temperature and at the temperature at which the peak frequency was attained.

2.4.2. Polymodal nociceptors

Spontaneous activity: Incidence (percentage of terminals firing more than 1 impulse during the initial 2 minutes of recording) and mean frequency of the spontaneous firing (imp·s^{-1}). *Amplitude of the stimulus response*: Total number of NTIs evoked by a particular stimulus (heat and capsaicin).

2.5. NTI waveform analysis

The following parameters from individual NTIs of cold thermoreceptor and polymodal nociceptor endings were measured: *Baseline:* Voltage value during a 10-millisecond period before the onset of the NTI. *Peak positive amplitude:* Maximum voltage of the NTI in reference to baseline. *Peak negative amplitude:* Minimum voltage of the NTI in reference to baseline. *Onset of the NTI:* Point in the NTI trace at which voltage increased to a value that was the baseline voltage plus 3 times its standard deviation. *Upstroke slope:* Change in voltage (*dV/dt*) between the onset of the NTI and the peak. *Downstroke slope:* Change in voltage (*dV/dt*) between the positive peak and the onset voltage value of the NTI. *Ratio between slopes:* Quotient between the upstroke and the downstroke slopes of the NTI. A minimum of 7 consecutive NTIs were measured and averaged to obtain the corresponding parameter of the waveform. NTIs were exported from raw data recordings without low- or high-pass filtering to prevent distortion of the NTI waveform shape. Control waveform was determined using NTIs recorded at the basal temperature of ~33.6°C and osmolality of 309 mOsm.L^{-1}. Waveform changes induced by hyperosmolal solutions were also measured just before application of a cooling ramp, 5 minutes after the onset of the perfusion with the test solution.

In addition, 23 consecutive NTI traces taken from the raw recordings of NTIs in different experimental conditions were averaged to obtain an averaged NTI waveform. The onset of the NTI was used for synchronization. Voltage values of each NTI were then taken between −0.26 milliseconds and +2.2 milliseconds around the onset value. Averaged NTIs are represented in the figures either conventionally, as time-dependent change of voltage, or as a phase–plane plot, in which the time derivative of the voltage (dV/dt) is plotted against the voltage [4,40].

2.6. Analysis of data

Data from NTI recordings were exported from Spike 2 (CED) to Origin 8 software for analysis. Statistical comparisons were performed using Microsoft Excel 2003, Origin 8 (OriginLab Corporation, Northampton, MA) and GraphPad Prism 5 software (GraphPad Software Inc, La Jolla, CA), selecting in each case the appropriate test, according to the characteristics of the data pool

and to data distribution. Data are expressed as mean ± standard error of the mean, with "n" denoting the number of terminals.

2.7. Solutions and drugs

Hyperosmolal solutions were prepared by adding NaCl (5 mol/L) to control saline solution. Actual osmolality was measured afterwards with a freezing point osmometer (Osmomat 030, Gonotec, Berlin, Germany). Final osmolality of the tested solutions was 311 ± 0.6 mOsm, 323 ± 0.9 mOsm, 343 ± 1.2 mOsm, 363 ± 2.0 mOsm, 403 ± 1.4 mOsm, and 464 ± 3.8 mOsm in experiments involving cold thermoreceptor recordings. Osmolality values in experiments involving polymodal nociceptors were as follows: 309.5 ± 0.6 mOsm, 363 ± 1.4 mOsm, 433 ± 13.4 mOsm, 608 ± 2.9 mOsm, 846 ± 9.2 mOsm, and 1005 ± 4.9 mOsm.

The inflammatory soup [35,45,64] contained the following substances dissolved in iso-osmolal or hyperosmolal saline solutions (final concentration in brackets): bradykinin (5 μmol/L), histamine (100 μmol/L), PGE_2 (10 μmol/L), serotonin (100 μmol/L), and ATP (100 μmol/L) (Sigma-Aldrich, St. Louis, MO).

3. Results

3.1. Cold thermoreceptors

3.1.1. Osmolality effects on NTI firing

Cold thermoreceptor endings were identified by their regular ongoing NTI activity at the basal bath temperature of 33.6°C, which increased markedly when the temperature of the flowing saline solution was suddenly decreased (Fig. 1).

The mean value of NTI frequency when perfusing with iso-osmolal solution at a mean basal temperature of 33.6°C ± 0.1°C, was 6.6 ± 1.0 imp·s^{-1} with extreme values ranging from 1.7 to 19.3 imp·s^{-1} (n = 20). In response to cooling ramps from 33.6°C ± 0.1°C to 16.9°C ± 0.4°C at a rate of 0.7°C ± 0.06°C·s^{-1}, NTI firing frequency increased significantly at an average threshold temperature of 31.9°C ± 0.3°C, with a change in firing rate of 5.5 ± 0.9 imp·s^{-1} per°C, and a mean peak frequency value of 57.1 ± 3.6 imp·s^{-1} attained at 24.6°C ± 0.9°C.

Fig. 1 shows an example of the effect of solutions of increasing osmolality on the NTI activity of a cold thermoreceptor terminal, showing the increase in background NTI activity and the change in firing pattern from a predominantly beating to bursting mode (see instantaneous frequency trace, Fig. 1A, middle trace) caused by high osmolality.

Fig. 2 represents the relationship between osmolality increases of the perfusing solution at 33.6°C and the increase in spontaneous firing rate of 26 cold-sensitive terminals. Increasing osmolality linearly augmented the ongoing firing frequency (R^2 = 0.499) at a mean rate of 0.35 imp·s^{-1} per 10 mOsm (y = −0.0304 + 0.0345x).

When mean firing frequency values before and after perfusion with hyperosmolal solutions were compared for each individual terminal, differences were significant during perfusion with 343 mOsm and over (325 mOsm: n = 5, P = .96, paired t test; 343 mOsm: n = 6, P = .038, paired t test; 363 mOsm: n = 6, P = .009, paired t test; 403 mOsm: n = 7, P = .015, Wilcoxon rank test; 464 mOsm: n = 8, P = .0003, paired t test).

To evaluate the influence of osmolality on dynamic cold responses, the change in cold threshold and in the maximal peak frequency evoked by cooling ramps (33.6°C to 16.9°C) during exposure to increasing osmolality levels was measured in 11 terminals. No significant changes in either of these parameters were observed even for high osmolality values (Table 1). Likewise, the slope of the NTI frequency variation as a function of temperature did not vary significantly for cooling ramps performed in increasingly

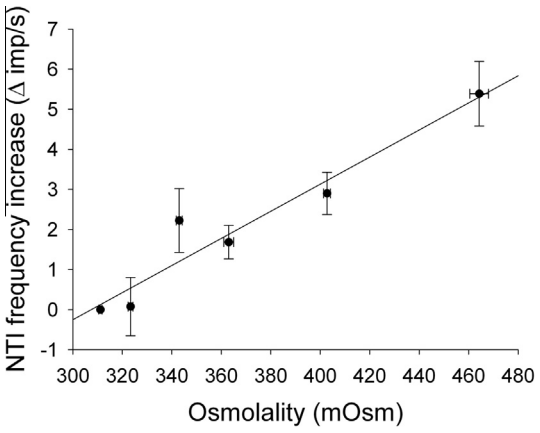

Fig. 2. Average change in nerve terminal impulse (NTI) activity of cold thermoreceptor endings caused by exposure to hyperosmotic solutions. Data are expressed as the change in mean frequency during exposure to a given hyperosmolal solution in relation to the mean firing frequency in the immediately preceding iso-osmolal conditions, measured in 26 corneal cold terminals. Pearson product moment analysis correlation coefficient = 0.707, P < .001. The average values of osmolality (mean ± standard error of the mean) for each point are as follows: 311 ± 0.6 mOsm, n = 9; 323 ± 0.9 mOsm, n = 9; 343 ± 1.2 mOsm, n = 6; 363 ± 1.9 mOsm, n = 6; 403 ± 1.4 mOsm, n = 7; and 464 ± 3.8 mOsm, n = 8.

hyperosmolal solutions (Table 1). This is also illustrated in Fig. 3, which depicts the mean firing frequency curves evoked by cooling ramps performed before and during perfusion with solutions of different osmolality. As mentioned above, the ongoing activity at the control temperature of 33.6°C under hyperosmolal solutions was higher than during previous perfusion with iso-osmolal solutions. The frequency curves evoked by the cooling ramp were rather variable, but no obvious differences in peak frequency value or dynamic firing during the initial temperature fall were associated with osmolality. Nonetheless, during exposure to osmolality solutions greater than 400 mOsm, the NTI firing pattern during the cooling ramp became more irregular, which is reflected in the distorted shape of the mean frequency curves (Fig. 3).

To further analyze the influence of osmolality on corneal cold thermoreceptor activity at different temperatures, we compared the firing response to staircase cooling (33.6°C to 21.6°C in drops of −3°C, 2.5 minutes per step, under iso- and hyperosmolal conditions). As illustrated in the example of Fig. 4A, exposure to hyperosmolal solutions markedly modified the NTI firing frequency and pattern of corneal cold nerve endings, in particular during the low temperature steps and with osmolality values greater than 363 mOsm. The samples of direct recordings of NTIs depicted in Fig. 4A exemplify these disturbances in firing pattern: Impulse firing became irregular, exhibiting paroxysmal discharges and silent periods, in particular at low temperatures and osmolality values greater than 403 mOsm, thereby causing large variations in mean firing frequency. This was reflected in the plateau of the stimulus–response curve, obtained when the mean firing frequency measured during the static part (last 30 seconds) of the cooling step was plotted against the temperature value of the step (Fig. 4B). Differences with stepwise cooling performed under iso-osmolal conditions became significant only during application of 363-mOsm solutions (receiver operating characteristic curve, P = .04).

3.1.2. Osmolality effects on NTI waveform

As shown in the direct recordings of NTIs shown in Fig. 1, exposure to hyperosmolal solutions decreased reversibly the amplitude of the NTIs. This amplitude reduction was more marked with osmolality values greater than 500 mOsm, at which the signal

Table 1
Parameters of the response to a cooling ramp performed under different osmolality conditions.

Osmolality (mOsm)	Spontaneous activity (impulses s^{-1})	Cooling threshold (−Δ°C)	Peak frequency (impulses s^{-1})	Slope (impulses $s^{-1}°C^{-1}$)
309	5.8 ± 1.9	1.3 ± 0.5	51.5 ± 7.2	7.7 ± 2.4
363	7.5 ± 2.2**	1.2 ± 0.6	56.7 ± 1.9	8.0 ± 1.6
403	11.0 ± 3.3*	1.6 ± 1.0	66.9 ± 7.6	7.6 ± 1.0
464	10.6 ± 0.8***	2.0 ± 0.7	53.4 ± 6.0	6.0 ± 1.7

Data are mean ± standard error of the mean; n = 11. The parameter values obtained during perfusion with each osmolality have been compared with the values measured immediately before, during perfusion with iso-osmolal solution.
* $P < .05$, paired t test.
** $P < .01$, paired t test.
*** $P < .001$, paired t test.

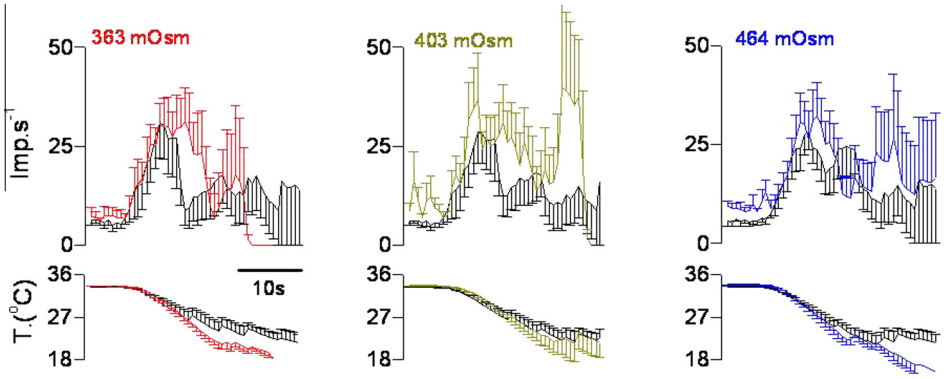

Fig. 3. Average response of cold thermoreceptors to cooling ramps performed at different osmolality levels. The mean change in firing frequency (imp s^{-1}, upper traces) evoked by a cooling ramp (°C, lower traces) of cold-sensitive terminals has been represented during perfusion with iso-osmolal solution (311 mOsm, black curves) and after shifting to perfusion with solutions of increasing osmolality (colored curves): 363 mOsm, n = 6; 403 mOsm, n = 7; 464 mOsm, n = 9. Data are mean ± standard error of the mean. Time scale: 10 seconds.

was frequently lost, although it recovered after washing (data not shown). This reduction limited our ability to study in cold thermoreceptor terminals the effects of solutions of high osmolality. Fig. 5A displays the change in NTI waveform at 33.6°C in the mean NTIs obtained from averaging 23 NTIs under solutions of increasing osmolality up to 464 mOsm. Around this value, NTIs were clearly of smaller amplitude, wider, and slower, although the ratio between slopes (see Methods) of the NTI remained unchanged (Table 2). In Fig. 5B, the spike potential V is displayed against its first time derivative dV/dt, as a phase–plane plot. In this representation, the slope of the response is represented for the complete NTI. The inflexion points where [dV/dt] reaches maximal values have been marked with arrows in the curve, and correspond to the maximal rate of rise and fall of the NTIs recorded under different osmolality values. This graphical representation visualizes membrane currents flowing during the NTI, showing that they were markedly reduced during exposure to hyperosmolal solutions (Fig. 5B).

3.1.3. Combined effects of hyperosmolality and cooling

We next tried to estimate the dynamic change in cold thermoreceptor firing occurring during the interblink temperature drop when tear fluid osmolality is high, as occurs in DED patients. We measured, in 6 cold thermoreceptor endings, the change in NTI impulse activity that occured at osmolalities of 325, 343, and 363 mOsm and corneal temperature drops of 1.8 ± 0.1°C (from 33.5°C to 31.7°C). Fig. 6A represents the firing frequency change caused by this dynamic temperature reduction under perfusion with the different hyperosmotic solutions and those obtained immediately before under iso-osmolal conditions. Mean firing frequency at 33.5°C under iso-osmolal conditions before exposure to the different hyperosmolality values did not vary (mean = 7.9 ± 0.9 imp·s^{-1}). As expected, a significant increase of the firing response to a temperature drop of 1.8°C was observed in these recordings, performed before exposure to each of the different hyperosmolal solutions (mean = 13.3 ± 1.4 imp·s^{-1}; $P < .001$, Wilcoxon signed-rank test). With exposure to hyperosmolal solutions, basal frequency at 33.6°C was significantly different from its iso-osmolal control when hyperosmolality exceeded 343 mOsm ($P < .05$, paired t test). Likewise, the 1.8°C ± 0.1°C cooling step further raised the firing rate response to values significantly higher than those seen with iso-osmolal conditions, with exposure to the 343 mOsm and 363 mOsm ($P < .01$, paired t test) but not with lower osmolality values (325 mOsm) (Fig. 6). Based on these observations, it can be postulated that, under moderate to high evaporation conditions leading to hyperosmolality levels of 340 and 360 mOsm and temperature drops around 1.8°C during the interblink period, 30% and 56% of the thermoreceptor firing frequency increase would be respectively attributable to the rise in osmolality, and 70% and 44% respectively to the temperature fall caused by evaporative cooling (Fig. 6B). Accordingly, augmented osmolality of the precorneal film and enhanced evaporative cooling appear to contribute jointly to generate high frequency firing rate of corneal cold thermoreceptors during dry eye conditions.

3.2. Polymodal nociceptors

Polymodal endings were identified by their very low spontaneous firing at rest, decreased activity during cooling ramps, activation by heat pulses, and 1 μmol/L capsaicin and mechanical responsiveness to gentle electrode displacements [7] (Fig. 7).

Fig. 8 represents the change in background impulse activity of 23 polymodal nociceptor terminals caused by perfusion of the cornea with solutions of increasing osmolality (363, 433, 608, 846, and 1005 mOsm). Significant elevations of mean impulse frequency were observed only with values greater than 600 mOsm (Fig. 8). At this and higher concentrations, impulse firing was

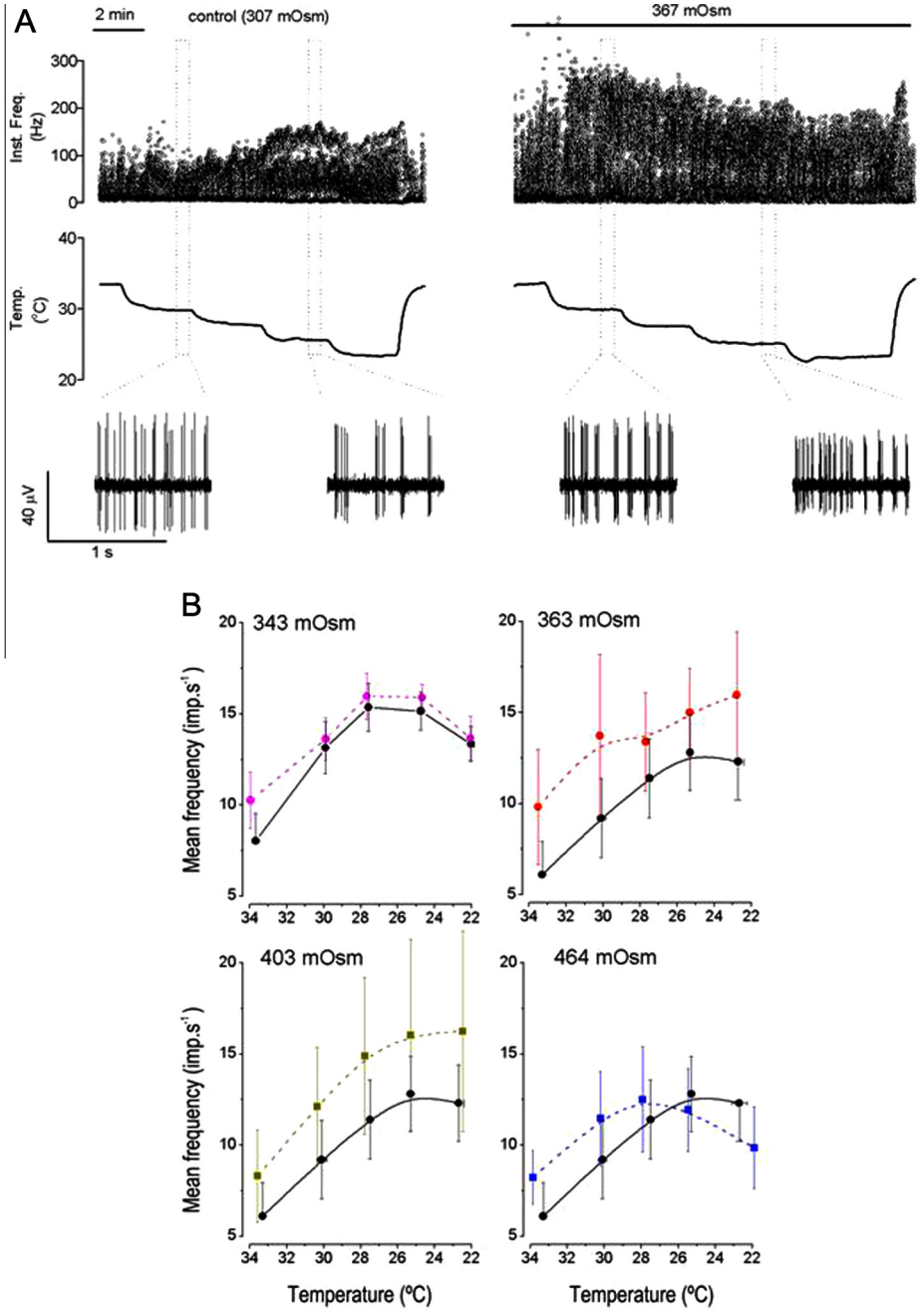

Fig. 4. Effect of hyperosmolality on corneal cold thermoreceptor response to staircase cooling. (A) Sample record of the nerve terminal impulse (NTI) response of a cold thermoreceptor ending to stepwise cooling (33°C to 23°C in 2.5°C steps) in iso-smolal conditions and after exposure to a hyperosmolal solution (367 mOsm). Perfusion with the hyperosmolal solution was started 10 minutes before the onset of the staircase cooling. Upper trace, instantaneous frequency (Hz); lower trace, bath temperature (°C). Sample recordings shown below are expanded views of the NTIs fired by the ending during the periods of time marked between dashed lines. Notice the irregular firing pattern during the third temperature step. (B) Mean NTI firing frequency during the last 30 seconds of the cooling step obtained from 6 corneal cold terminals perfused with iso-osmolal solution (black traces) and exposed to 4 hyperosmolal conditions (colored traces). Data are mean ± SEM. Activity under 363 mOsm was significantly different from the control solution (receiver operating characteristic curve, $P = .04$).

irregular, with occasional paroxysmal discharges. This was reflected in a different distribution of the duration of impulse intervals after exposure to high osmolality (Fig. 7A, Instantaneous frequency channel). The shape of NTIs was also altered during exposure to high osmolality solutions, with NTIs becoming flattened and slower (Table 3), particularly during the downstroke component (Fig. 9A). Current flow reduction was also evident in the phase–plane plot of the averaged NTIs (Fig. 9B).

To determine whether sensitivity of polymodal nociceptors to hyperosmolal solutions was modified by previous sensitization, perfusion with an inflammatory soup [45] (see Methods) dissolved in iso-osmolal saline was initiated 5 minutes before shifting to the higher osmolality solutions plus inflammatory soup. Sensitization of polymodal nociceptors, including corneal polymodal nociceptors, by this particular mixture of inflammatory mediators has been repeatedly established [35,64]. Perfusion with the inflammatory soup in iso-osmolal saline at 33.6°C increased significantly the frequency of the spontaneous activity (from 0.10 ± 0.2 imp·s^{-1} to 0.19 ± 0.04 imp·s^{-1}, n = 7; $P = .003$, paired t test). This higher activity did not further increase when perfusion with the inflammatory soup in iso-osmolal solution was shifted to hyperosmolal solutions also containing the inflammatory soup (370 mOsm

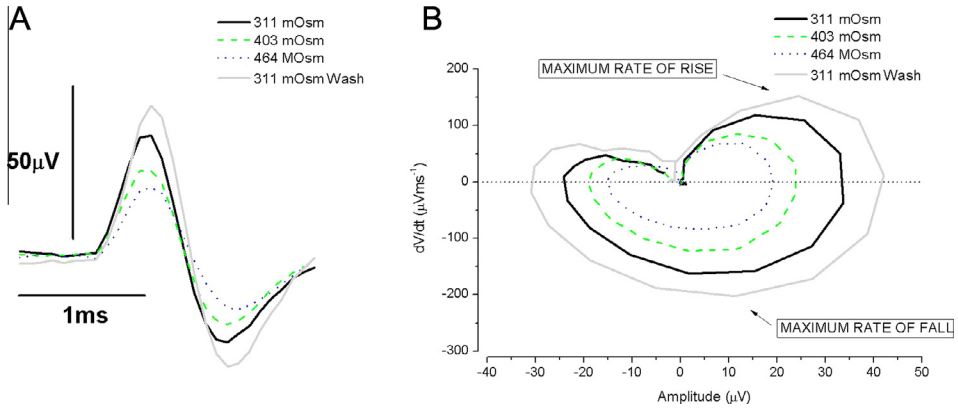

Fig. 5. Change in nerve terminal impulse (NTI) waveform of cold thermoreceptor terminals during exposure to hyperosmolal solutions. (A) Each trace is the average of 23 NTIs exported from the different segments of the recording shown in Fig. 1. (B) Phase–plane plots of the average NTIs are shown in A. Arrows indicate the points of maximal rate of rise or fall of currents generating NTIs.

Table 2
NTI waveform parameters at different osmolality values at basal temperature (33.5°C).

Osmolality (mOsm)	Peak positive amplitude (μV)	Peak negative amplitude (μV)	Total amplitude (μV)	Up-stroke slope (μV·ms^{-1})	Down-stroke slope (μV·ms^{-1})	Ratio between slopes
309	41.2 ± 1.2	−28.4 ± 1.0	69.6 ± 2.1	143.0 ± 5.5	177.8 ± 7.0	0.83 ± 0.02
363	32.9 ± 2.1***	−23.0 ± 1.6	55.8 ± 3.5**	119.8 ± 9.6	154.1 ± 12.2	0.80 ± 0.04
403	35.3 ± 1.6*	−22.6 ± 1.3	57.9 ± 2.7*	130.0 ± 8.5	163.0 ± 8.6	0.80 ± 0.03
464	24.1 ± 0.9***	−16.1 ± 0.2***	40.2 ± 1.4***	85.1 ± 5.6***	100.9 ± 5.6***	0.87 ± 0.04

NTI, nerve terminal impulse.
Data are mean ± standard error of the mean; n = number of terminals.
For each terminal, the different parameters were calculated from 7 individual NTIs recorded under different osmolality conditions.
* $P < .05$, n = 6; paired t test, difference from the values at 309 mOsm.
** $P < .01$, n = 7; paired t test, difference from the values at 309 mOsm.
*** $P < .001$, n = 8; paired t test, difference from the values at 309 mOsm.

[0.18 ± 0.04 imp·s^{-1}, n = 3] or 490 mOsm [0.17 ± 0.04 imp·s^{-1}, n = 3]. One unit treated with the inflammatory soup did not show sensitization and was not included in the analysis.

4. Discussion

Our results show that exposure of the mouse eye surface to NaCl solutions, bringing ocular surface osmolality to the values found in experimentally induced eye dryness in this species [56], augmented NTI activity of corneal sensory afferents. Corneal cold thermoreceptor endings were more sensitive and responded more prominently to osmolality increases than corneal polymodal nociceptor endings. Altogether, our data suggest that high tear osmolality values, such as those usually reported in DED patients (20%–30% above the normal value of ~300 mOsm measured at the tear meniscus) predominantly affect cold thermoreceptor activity, whereas nociceptors are additionally recruited only if much higher hyperosmolality levels are attained.

The regional variations of tear fluid osmolality at the ocular surface occurring during normal and pathological circumstances are complex and not known in detail [66]. When tear fluid osmolality is used for DED clinical evaluation, only mean values measured in the fluid accumulated at the asymmetrical menisci adjacent to the upper and lower eyelid margins are considered [57]. However, in the exposed areas of the eye, the tear film is only a few microns thick, becoming thinnest at the transition interface between tear film and eye tissues. Moreover, tear film is subjected during each blink to a dynamic spreading that modifies its geometry [29,63,66]. These factors affect the evaporation rate and thereby osmolality values. Hence, changes in solute concentration caused by evaporation and diffusion do not distribute homogeneously across the ocular surface, and actual osmolality may be much higher than average values in certain regions of the eye surface. For instance, in zones such as the black lines (local thinning regions near lids), where evaporation rates are normally faster, relative osmolality concentrations rise in normal individuals to values close to those measured in clinical dry eye [16,29]. The expected heterogeneity of osmolal values across the ocular surface is aggravated under enhanced evaporation conditions, as is the case in evaporative dry eyes, in which tear osmolality reaches mean values of 365 mOsm in individual patients [29], and perhaps much higher transient hyperosmolality peaks [48]. Moreover, lachrymal gland or meibomian gland secretory dysfunctions, contact lens wearing, and different keratopathies [23,27,30,55] may also lead to abnormally high tear fluid osmolality values.

Our work shows that increases of osmolality within the above mentioned margins already affect nerve impulse firing in some ocular sensory fibers. This is not surprising, considering that osmolality changes in the tear film extend rapidly to the extracellular fluid around the uppermost corneal and conjunctival epithelium cell layers, where sensory nerve branches innervating these tissues are located, thus modifying the osmolality of the fluid around their nerve terminals. Expectedly, individual terminals are not equally exposed to osmolal changes, explaining the variability in the effect of moderate osmolal increments shown in Fig. 2. In addition, outward water movements across cell membranes of epithelial cells due to extreme elevations in osmolality probably induce shrinking of cells and endings [28], which may, in turn, act indirectly as mechanical stimuli.

Ion channels highly sensitive to hypo-osmolality have been reported in a fraction of mechanoreceptor and nociceptor sensory neurons. They include various members of the TRP family of

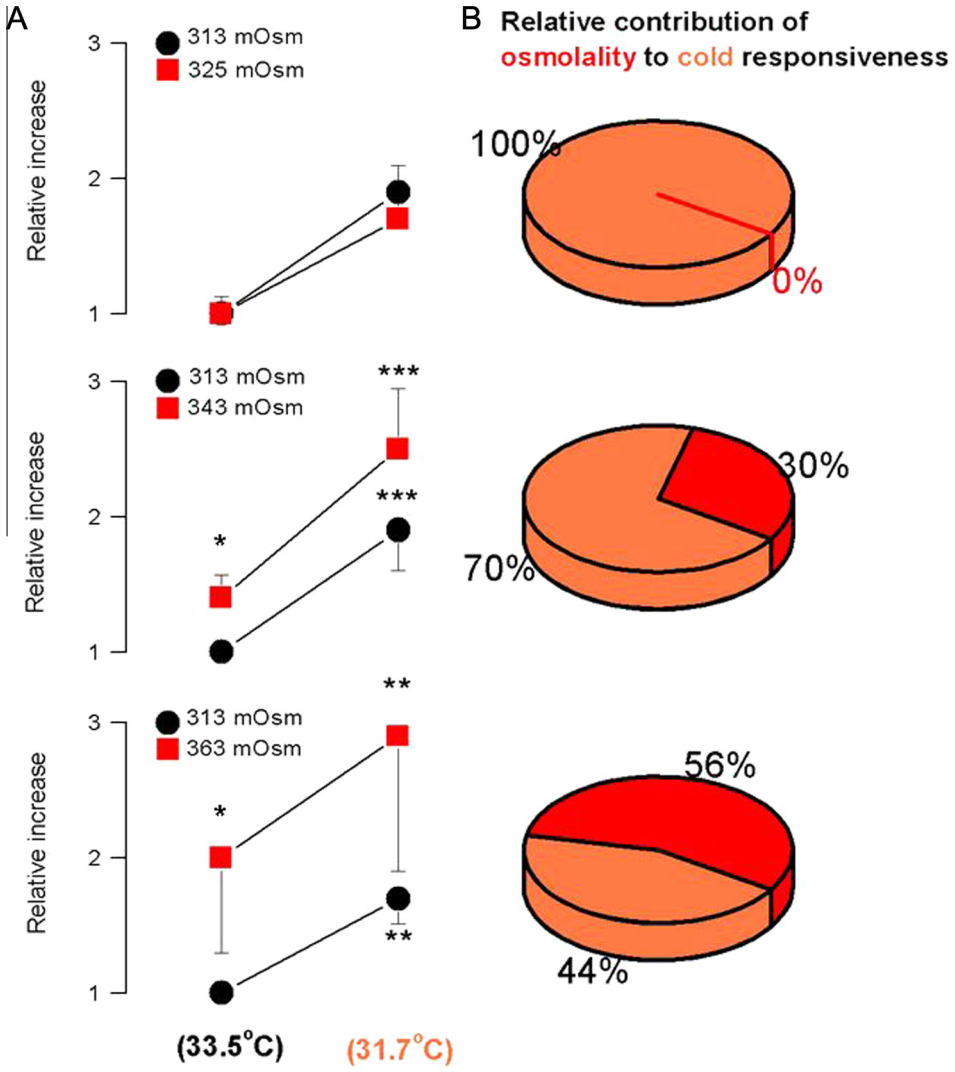

Fig. 6. Summation of cooling and hyperosmolality effects on the impulse firing of corneal cold thermoreceptors. (A) Mean firing frequency of 17 units was measured during the 30-second period preceding the onset of a cooling ramp from 33.5°C to 31.7°C, and during the first 30 seconds of the cooling period; the effect of cold and osmolality on the firing frequency was expressed for each hyperosmolality value as the relative increase in firing frequency from its value at 33.5°C under iso-osmolal conditions. Data are mean ± SEM, n = 6; paired *t* test, differences between osmolalities at 33.5°C (*$P < .05$) and at 31.7°C (**$P < .01$, ***$P < .001$). (B) Relative contribution of cooling (orange) and of osmolality (red) to the enhanced impulse response elicited when both conditions act simultaneously.

nonselective cationic channels, principally TRPV4, TRPC5, and TRPM3 [3,31,34]. Their final activation mechanism by osmolal changes is disputed, and may include membrane stretch acting either directly on the channel or through mechanosensitive G proteins that, in turn, open the channel via activation of second-messenger pathways. The final result is membrane depolarization and, ultimately, pain [2].

In contrast, experimental evidence supporting the existence of specific ion channels sensing expressed directly hypertonic solutions is scarce. Nonetheless, TRPA1 channels both in cell lines and in DRG nociceptive neurons are activated by moderately hyperosmolal (up to 400 mOsm) but not by hypo-osmolal solutions [65]. Also, activation of ASIC3 channels by acid in DRG nociceptive neurons is enhanced during exposure to hyperosmolal solutions (600 mOsm with mannitol) [20]. Cells heterologously expressing TRPM8 are respectively activated or inhibited by small osmolality increases and decreases around physiological levels [54]. This effect could explain mechanistically with the observed changes in firing activity of corneal cold thermoreceptors caused by hyperosmolal solutions. High concentrations of NaCl may also alter the behavior of ion channels in sensory nerve terminals through mechanisms other than an osmotic action. High concentrations of Na and Cl ions modify the surface charge of the membrane, modifying the surrounding ionic environment near the ion channels and offsetting the potential differences across them. This changes ion permeation as well as voltage-dependent processes such as gating and channel block [33,36,41].

We found that the background firing frequency of corneal cold receptors at 34°C was positively correlated with the osmolal concentration of the extracellular solution, with differences becoming significant at values greater than 340 mOsm. Comparatively, the parameters of the NTI firing response to dynamic cooling were less affected. A similar increase in cold background activity of cold receptors was obtained with hyperosmolal solutions of the same osmolality but prepared with mannitol [54], thus supporting the view that the effect is mediated at least in part through osmotic activation of TRPM8, the transduction channel critical for background and cold-evoked activity in corneal cold thermoreceptors [53]. The comparatively low sensitivity of polymodal nociceptors when exposed to solutions of similar hyperosmolality further favors the interpretation that TRPM8 channels contribute to the sensitivity of cold thermoreceptors to moderate hyperosmolality. Hyperosmolal concentrations exceeding values of 600 mOsm evoked an irregular, high-frequency impulse activity in both cold

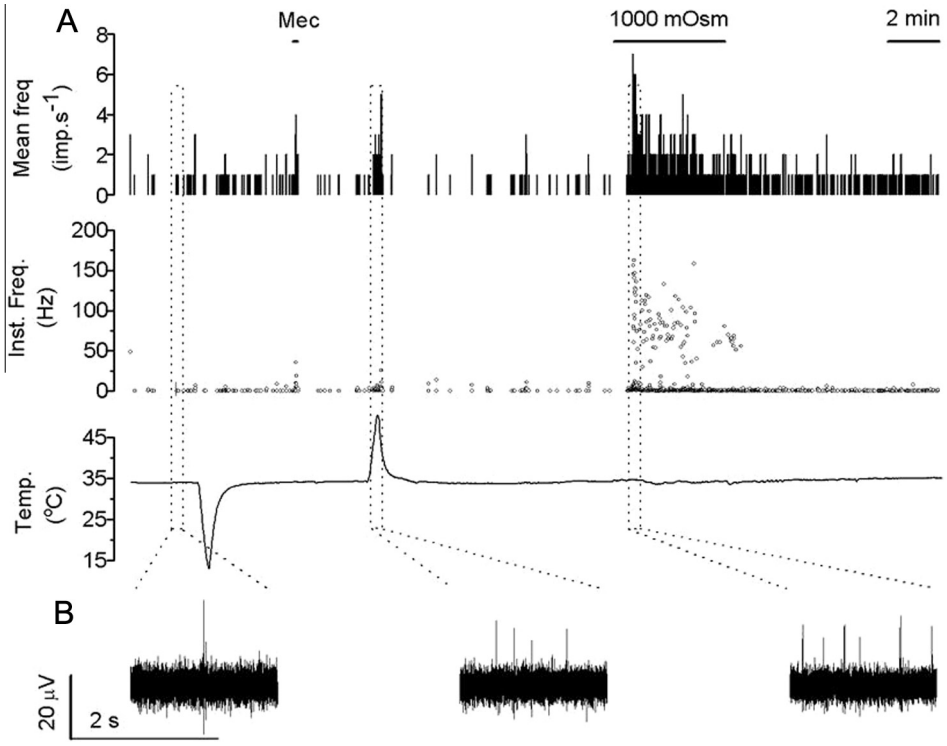

Fig. 7. Effect of hyperosmolality on polymodal nociceptor activity. (A) Response of a polymodal nociceptor terminal to a cooling ramp, a heating ramp (to 50.0°C), mechanical stimulation (Mec) performed with a microelectrode displacement, and perfusion with a hyperosmolal NaCl solution. Upper trace, mean firing rate (imp·s^{-1}); middle trace, instantaneous frequency (Hz); lower trace, bath temperature (°C). (B) Sample recordings showing an expanded view of the nerve terminal impulse (NTIs) fired during the periods marked between the dashed lines.

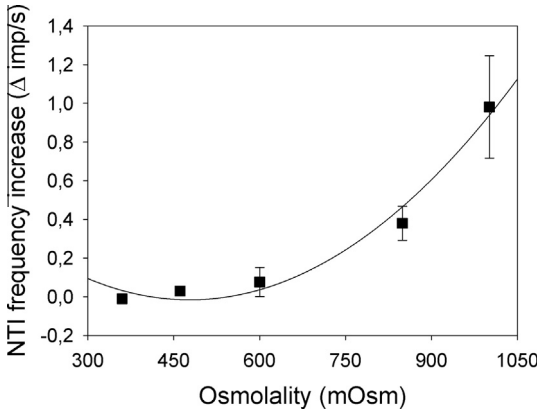

Fig. 8. Average change in nerve terminal impulse (NTI) activity of polymodal nociceptor terminals obtained during perfusion with solutions of increasing osmolality. Data are expressed as the change in mean frequency during exposure to a given hyperosmolal solution in relation to the mean firing frequency during the immediately preceding iso-osmolal conditions. The line corresponds to the linear second-order regression line ($R^2 = 0.6125$).

and polymodal receptor endings, possibly reflecting nonspecific disturbances in membrane potential currents.

The shape of NTIs of cold thermoreceptors and polymodal nociceptors recorded extracellularly in corneal nerve terminals was also markedly affected by hyperosmolality. NTIs amplitude and shape are determined by the currents generated by propagated action potentials, depending on regenerative Na^+ currents and local electrotonic currents [6,13,14,17]. Phase–plane plots of NTIs reflected a reduction in the rates of spike rise and fall and in the amplitude of the negative after-potential, all of which were more prominent in cold thermoreceptors than in polymodal nociceptors. This likely reflects a decrease in maximal outward and inward currents at the endings [40], which are possibly the consequence of an altered activation of voltage-gated channels, transducing channels, and/or channels involved in the regulation of background neuronal excitability [12,32].

In human beings with dry eye conditions, corneal temperatures are often below 34°C [44], whereas tear osmolality is high [10,16,25,57,61]. Under hyperosmolal conditions in mice, we found that background firing frequency of cold thermoreceptors at the normal corneal temperature around 34°C was higher than normal. Moreover, the overall cold thermoreceptor activity during experimental dynamic temperature drops, resembling those that occur at the ocular surface when eyes remain open, increased markedly when osmolality was also high.

In human DED, temperature and osmolality oscillations are heterogeneous, fluctuant, and often combined with chronic inflammation. Hence, extrapolation of the experimental data obtained in the mouse cornea in vitro to human patients with DED has to be made with caution, especially because the effects of long-term exposure of nerve endings to hyperosmolal conditions are still unexplored. Still, it seems reasonable to assume that disturbances of corneal cold thermoreceptor activity in mice caused by hyperosmolal solutions also develop in DED patients. Such augmented afferent impulse activity from cold thermoreceptors represents a stronger neural input to stimulate basal tear secretion by the lachrymal glands [53] and may also evoke conscious cooling sensations that, in addition, include feelings of discomfort and dryness [1,46]. The enhanced firing of cold thermoreceptors observed when the stimulatory action of cold and hyperosmolality are combined reinforces the hypothesis that this population of thermal sensory receptors contributes importantly to the unpleasant sensations reported by DED patients [8]. In contrast, direct activation of polymodal nociceptors by hyperosmolal tears within the range usually found in DED patients possibly plays a minor role in evoking the unpleasant sensations experienced in this disease, although their recruitment

Table 3
NTI waveform parameters of polymodal nociceptors at different osmolality averaged values.

Osmolality (mOsm)	Peak positive amplitude (μV)	Peak negative amplitude (μV)	Total amplitude (μV)	Up-stroke slope (μV ms^{-1})	Down-stroke slope (μV ms^{-1})	Ratio of slopes
309	25.9 ± 0.7	−11.4 ± 0.8	37.3 ± 0.1	48.6 ± 2.1	54.5 ± 2.2	0.9 ± 0.05
363	29.2 ± 1.1	−6.1 ± 1.4	35.3 ± 1.7	51.1 ± 3.5	44.4 ± 2.8	1.23 ± 0.14
433	22.6 ± 1.0	−16.1 ± 1.0	38.7 ± 1.4	65.5 ± 5.3	53.6 ± 3.2	1.25 ± 0.12
608	24.7 ± 0.8	−1.2 ± 1.2**	25.9 ± 0.7**	37.4 ± 2.5	36.2 ± 2.6 *	1.07 ± 0.08
846	18.4 ± 0.8**	−5.9 ± 1.4**	24.3 ± 1.5***	41.1 ± 2.5*	31.8 ± 1.5***	1.33 ± 0.12
1005	16.6 ± 0.6***	−5.4 ± 1.0***	22.0 ± 1.0**	34.8 ± 2.3	33.4 ± 1.0**	1.05 ± 0.09

NTI, nerve terminal impulse.
Data from 10 consecutive NTIs of each unit (n = 10) were averaged for each osmolality value.
* $P < .05$; paired t test, difference from the value under its iso-osmolal conditions (309 mOsm).
** $P < .01$; paired t test, difference from the value under its iso-osmolal conditions (309 mOsm).
*** $P < .001$; paired t test, difference from the value under its iso-osmolal conditions (309 mOsm).

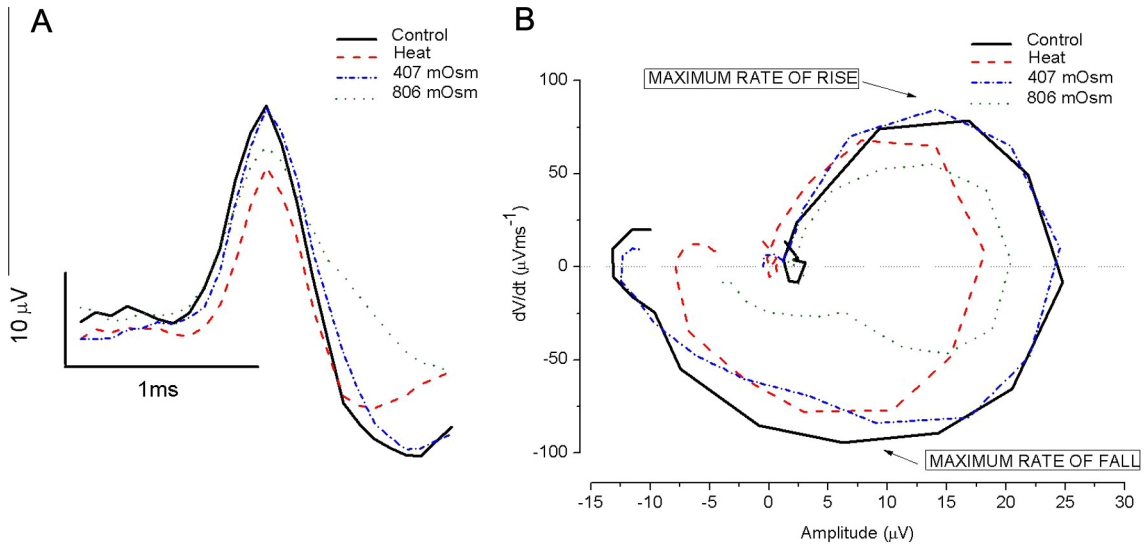

Fig. 9. Average change in waveform of the nerve terminal impulse (NTIs) fired by a corneal polymodal nerve ending during exposure to hyperosmolal solutions and to heating. Each wave is the average of 10 NTIs exported from the corresponding segments of the recording. The NTIs used for the graphs A and B are the same. (A) Data are expressed as the change of voltage in respect to time. (B) Data for the same NTIs are represented as a phase–plane plot as in Fig. 5.

by transient, very high osmolality peaks [48] cannot be excluded. Although it is likely that polymodal nociceptors become sensitized by the release of inflammatory mediators resulting from osmotic stress on corneal surface cells [62], hyperosmolality does not seem to contribute additionally to the enhanced responsiveness of polymodal nerve endings. Nonetheless, disturbances of polymodal nociceptor activity due to long-term inflammation or to neuropathic disturbances [21,51] can be expected to contribute to the total peripheral sensory inflow leading to discomfort.

4.1. Conclusion

In conclusion, this work provides evidence that increases in tear osmolality accompanying evaporative dryness of the eye surface act as an effective stimulus, particularly for the population of ocular cold thermoreceptor nerve fibers. Cooling and hyperosmolality summate to build up an augmented sensory inflow to the brain that, under chronic conditions such as those usually developed by patients with DED, contributes to the augmented blinking, disturbed tearing, and conscious sensations of discomfort and dryness characteristic of this disease.

Conflict of interest statement

No author has any conflict of interest related to the content of this article.

Acknowledgements

The authors thank Eva Quintero, Enol Artime, and Susana Quirce for technical support; Drs. Roberto Gallego, Felix Viana, and Stuart Bevan for critical reading of the manuscript; and Dr. Jesus Merayo-Lloves for continuous collaboration. This work was supported by grant BFU2008-04425 and in part by CSD2007-00023 and SAF2011-22500 from Ministerio de Economía y Competitividad, Spain, and by Fundación Mª Cristina Masaveu Peterson - Spain.

References

[1] Acosta MC, Belmonte C, Gallar J. Sensory experiences in humans and single unit activity in cats evoked by polymodal stimulation of the cornea. J Physiol 2001;534:511–25.
[2] Alessandri-Haber N, Dina OA, Chen X, Levine JD. TRPC1 and TRPC6 channels cooperate with TRPV4 to mediate mechanical hyperalgesia and nociceptor sensitization. J Neurosci 2009;29:6217–28.
[3] Alessandri-Haber N, Yeh JJ, Boyd AE, Parada CA, Chen X, Reichling DB, Levine JD. Hypotonicity induces TRPV4-mediated nociception in rat. Neuron 2003;39:497–511.
[4] Bean BP. The action potential in mammalian central neurons. Nat Rev Neurosci 2007;8:451–65.
[5] Belmonte C, Aracil A, Acosta MC, Luna C, Gallar J. Nerves and sensations from the eye surface. Ocul Surf 2004;2:248–53.
[6] Belmonte C, Brock JA, Viana F. Converting cold into pain. Exp Brain Res 2009;196:13–30.
[7] Belmonte C, Gallar J, Pozo MA, Rebollo I. Excitation by irritant chemical substances of sensory afferent units in the cat's cornea. J Physiol 1991;437:709–25.

[8] Belmonte C, Gallar J. Cold thermoreceptors, unexpected players in tear production and ocular dryness sensations. Invest Ophthalmol Vis Sci 2011;52:3888–92.
[9] Belmonte C, Giraldez F. Responses of cat corneal sensory receptors to mechanical and thermal stimulation. J Physiol 1981;321:355–68.
[10] Benjamin WJ, Hill RM. Human tears: Osmotic characteristics. Invest Ophthalmol Vis Sci 1983;24:1624–6.
[11] Borchman D, Foulks GN, Yappert MC, Mathews J, Leake K, Bell J. Factors affecting evaporation rates of tear film components measured in vitro. Eye Contact Lens 2009;35:32–7.
[12] Brickley SG, Aller MI, Sandu C, Veale EL, Alder FG, Sambi H, Mathie A, Wisden W. TASK-3 two-pore domain potassium channels enable sustained high-frequency firing in cerebellar granule neurons. J Neurosci 2007;27:9329–40.
[13] Brock J, McLachlan EM, Belmonte C. Tetrodotoxin-resistant impulses in single nociceptor nerve terminals in guinea-pig corneas. J Physiol 1998;512:211–7.
[14] Brock JA, Pianova S, Belmonte C. Differences between nerve terminal impulses of polymodal nociceptors and cold sensory receptors of the guinea-pig cornea. J Physiol 2001;533:493–501.
[15] Bron AJ, Tiffany JM, Gouveia SM, Yokoi N, Voon LW. Functional aspects of the tear film lipid layer. Exp Eye Res 2004;78:347–60.
[16] Bron AJ, Yokoi N, Gaffney EA, Tiffany JM. A solute gradient in the tear meniscus. I. A hypothesis to explain Marx's line. Ocul Surf 2011;9:70–91.
[17] Carr RW, Pianova S, McKemy DD, Brock JA. Action potential initiation in the peripheral terminals of cold-sensitive neurons innervating the guinea pig cornea. J Physiol 2009;587:1249–64.
[18] Craig JP, Tomlinson A. Importance of the lipid layer in human tear film stability and evaporation. Optom Vis Sci 1997;74:8–13.
[19] Dartt DA. Formation and function of the tear film. In: Kaufman PL, Alm A, editors. Adler's physiology of the eye. Elsevier: Saunders; 2011. p. 350–62.
[20] Deval E, Noël J, Lay N, Alloui A, Diochot S, Friend V, Jodar M, Lazdunski M, Lingueglia E. ASIC3, a sensor of acidic and primary inflammatory pain. EMBO J 2008;27:3047–55.
[21] Devor M. Neuropathic pain: Pathophysiological response of nerves to injury. In: McMahon S, Koltzenburg M, Tracey I, Turk DC, editors. Wall & Melzack's textbook of pain. Philadelphia, PA: Elsevier; 2014. p. 861–88.
[22] Efron N, Young G, Brennan NA. Ocular surface temperature. Curr Eye Res 1989;8:901–6.
[23] Foulks GN. The correlation between the tear film lipid layer and dry eye disease. Surv Ophthalmol 2007;52:369–74.
[24] Franzco IC. Fluids of the ocular surface: Concepts, functions and physics. Clin Exp Ophthalmol 2012;40:634–43.
[25] Gaffney EA, Tiffany JM, Yokoi N, Bron AJ. A mass and solute balance model for tear volume and osmolality in the normal and the dry eye. Prog Retin Eye Res 2010;29:59–78.
[26] Gallar J, Pozo MA, Tuckett RP, Belmonte C. Response of sensory units with unmyelinated fibres to mechanical, thermal and chemical stimulation of the cat's cornea. J Physiol 1993;468:609–22.
[27] Gilbard JP. Human tear film electrolyte concentrations in health and dry-eye disease. Int Ophthalmol Clin 1994;34:27–36.
[28] Gilbard JP, Carter JB, Sang DN, Refojo MF, Hanninen LA, Kenyon KR. Morphologic effect of hyperosmolarity on rabbit corneal epithelium. Ophthalmology 1984;91:1205–12.
[29] Gilbard JP, Farris RL. Tear osmolality and ocular surface disease in keratoconjunctivitis sicca. Arch Ophthalmol. 1979;97:1642–6.
[30] Gilbard JP, Gray KL, Rossi SR. A proposed mechanism for increased tear-film osmolarity in contact lens wearers. Am J Ophthalmol 1986;102:505–7.
[31] Gomis A, Soriano S, Belmonte C, Viana F. Hypoosmotic- and pressure-induced membrane stretch activate TRPC5 channels. J Physiol 2008;586:5633–49.
[32] Gonzalez JA, Jensen LT, Doyle SE, Miranda-Anaya M, Menaker M, Fugger L, Bayliss DA, Burdakow D. Deletion of TASK1 and TASK3 channels disrupts intrinsic excitability but does not abolish glucose or pH responses of orexin/hypocretin neurons. Eur J Neurosci 2009;30:57–64.
[33] Green WN, Andersen OS. Surface charges and ion channel function. Annu Rev Physiol 1991;53:341–59.
[34] Grimm C, Kraft R, Sauerbruch S, Schultz G, Harteneck C. Molecular and functional characterization of the melastatin-related cation channel TRPM3. J Biol Chem 2003;278:21493–501.
[35] Handwerker HO, Reeh PW. Pain and inflammation. In: Bond MR, Charlton JB, Woolf CJ, editors. Pain research and clinical management. Proceedings of the VIth world congress on pain, vol. 4. Elsevier: Amsterdam; 1991. p. 59–70.
[36] Hille B. Ion channels of excitable membranes. Sunderland, MA: Sinauer Associates; 2002.
[37] Hirata H, Meng ID. Cold-sensitive corneal afferents respond to a variety of ocular stimuli central to tear production: implications for dry eye disease. Invest Ophthalmol Vis Sci 2010;51:3969–76.
[38] Hirata H, Okamoto K, Tashiro A, Bereiter DA. A novel class of neurons at the trigeminal subnucleus interpolaris/caudalis transition region monitors ocular surface fluid status and modulates tear production. J Neurosci 2004;24:4224–32.
[39] Iwata S, Lemp MA, Holly FJ, Dohlman CH. Evaporation rate of water from the precorneal tear film and cornea in the rabbit. Invest Ophthalmol 1969;8:613–9.
[40] Jenerick H. Phase plane trajectories of the muscle spike potential. Biophys J 1963;3:363–77.
[41] Jiang Y, Ruta V, Chen J, Lee A, MacKinnon R. The principle of gating charge movement in a voltage-dependent K+ channel. Nature 2003;423:42–8.
[42] Johnson ME. The association between symptoms of discomfort and signs in dry eye. Ocul Surf 2009;7:199–211.
[43] Julio G, Lluch S, Pujol P, Merindano MD. Effects of tear hyperosmolality on conjunctival cells in mild to moderate dry eye. Ophthalmic Physiol Opt 2012;32:317–23.
[44] Kamao T, Yamaguchi M, Kawasaki S, Mizoue S, Shiraishi A, Ohashi Y. Screening for dry eye with newly developed ocular surface thermographer. Am J Ophthalmol 2011;151:782–91.
[45] Kessler W, Kirchoff C, Reeh PW, Handwerker HO. Excitation of cutaneous afferent nerve endings in vitro by a combination of inflammatory mediators and conditioning effect of substance P. Exp Brain Res 1992;91:467–76.
[46] Kovács I, Luna C, Quirce S, Mizerska K, Callejo G, Riestra A, Fernández-Sánchez L Meseguer VM, Cuenca N, Merayo-Lloves J, Gasull X, Acosta MC, Belmonte C, Gallar J. Abnormal activity of corneal cold thermoreceptors underlies the unpleasant sensations in dry eye disease. Submitted for publication.
[47] Kurose M, Meng ID. Dry eye modifies the thermal and menthol responses in rat corneal primary afferent cool cells. J Neurophysiol 2013;110:495–504.
[48] Liu H, Begley C, Chen M, Bradley A, Bonanno J, McNamara NA, Nelson JD, Simpson T. A link between tear instability and hyperosmolality in dry eye. Invest Ophthalmol Vis Sci 2009;50:3671–9.
[49] McCulley JP, Uchiyama E, Aronowicz JD, Butovich IA. Impact of evaporation on aqueous tear loss. Trans Am Ophthalmol Soc 2006;104:121–8.
[50] Mengher LS, Pandher KS, Bron AJ. Non-invasive tear film break-up time: Sensitivity and specificity. Acta Ophthalmol 1986;64:441–4.
[51] Meyer RA, Campbell JN. Myelinated nociceptive afferents account for the hyperalgesia that follows a burn to the hand. Science 1981;213:1527–9.
[52] Mishima S, Maurice DM. The oily layer of the tear film and evaporation from the corneal surface. Exp Eye Res 1961;1:39–45.
[53] Parra A, Madrid R, Echevarria D, delOlmo S, Morenilla-Palao C, Acosta MC, Gallar J, Dhaka A, Viana F, Belmonte C. Ocular surface wetness is regulated by TRPM8-dependent cold thermoreceptors of the cornea. Nat Med 2010;16:1396–9.
[54] Quallo TE, Vastani N, Horridge E, Parra A, Zimmermann K, Gentry C, Viana F, Belmonte C, Andersson DA, Bevan S. TRPM8 acts as a sensor for increased osmolarity. Neuroscience Meeting Planner. San Diego, CA: Society for Neuroscience; 2013. Program No. 641.01. Nov. 9–13.
[55] Report of the International Dry eye Workshop. DEWS. Ocul Surf 2007;5:65–204.
[56] Stewart P, Chen Z, Farley W, Olmos L, Pflugfelder SC. Effect of experimental dry eye on tear sodium concentration in the mouse. Eye Contact Lens 2005;31:175–8.
[57] Sullivan BD, Whitmer D, Nichols KK, Tomlinson A, Foulks GN, Geerling G, Pepose JS, Kosheleff V, Porreco A, Lemp MA. An objective approach to dry eye disease severity. Invest Ophthalmol Vis Sci 2010;51:6125–30.
[58] Tan JH, Ng EYK, Acharya UR. Evaluation of tear evaporation from ocular surface by functional infrared thermography. Med Phys 2010;37:6022–34.
[59] Tashiro A, Okamoto K, Chang Z, Bereiter DA. Behavioral and neurophysiological correlates of nociception in an animal model of photokeratitis. Neuroscience 2010;169:455–62.
[60] Tomlinson A, Doane MG, McFadyen A. Inputs and outputs of the lacrimal system: Review of production and evaporative loss. Ocul Surf 2009;7:186–98.
[61] Tomlinson A, McCann LC, Pearce EI. Comparison of human tear film osmolality measured by electrical impedance and freezing point depression techniques. Cornea 2010;29:1036–41.
[62] Versura P, Profazio V, Schiavi C, Campos EC. Hyperosmolar stress upregulates HLA-DR expression in human conjunctival epithelium in dry eye patients and in vitro models. Invest Ophthalmol Vis Sci 2011;52:5488–96.
[63] Werkmeister RM, Alex A, Kaya S, Unterhuber A, Hofer B, Riedl J, Bronhagl M, Vietauer M, Schmidl D, Schmoll T, Garhöfer G, Drexler W, Leitgeb RA, Groeschl M, Schmetterer L. Measurement of tear film thickness using ultrahigh-resolution optical coherence tomography. Invest Ophthalmol Vis Sci 2013;54:5578–83.
[64] Zhang X, Mak S, Li L, Parra A, Denlinger B, Belmonte C, McNaughton PA. Direct inhibition of the cold-activated TRPM8 ion channel by Gαq. Nat Cell Biol 2012;14:851–8.
[65] Zhang XF, Chen J, Faltynek CR, Moreland RB, Neelands TR. Transient receptor potential A1 mediates an osmotically activated ion channel. Eur J Neurosci 2008;27:605–11.
[66] Zubkov VS, Breward CJ, Gaffney EA. Coupling fluid and solute dynamics within the ocular surface tear film: A modelling study of black line osmolality. Bull Math Biol 2012;74:2062–93.